

> REPLACE THIS LINE WITH YOUR MANUSCRIPT ID NUMBER (DOUBLE-CLICK HERE TO EDIT) <

# Moisture Content Estimation Models of Flour Matrices in the 67-110 GHz Frequency Range using a Non-Destructive and Contactless Monitoring System

Carlos Quemada Mayoral, Iñigo Ederra, *Member, IEEE*, Miguel Beruete, Ramón Gonzalo, *Member, IEEE*, and Juan Carlos Iriarte

**Abstract**— This work addresses the lack of moisture content estimation models for food products in the millimeter-wave frequency range and showcases the potential of this range for designing compact, cost-effective and in-line food moisture sensors. The moisture content estimation models developed in this study are intended for flour-based mixtures in the 67-110 GHz frequency range and are derived by means of a non-destructive and contactless monitoring system. To this aim, data obtained by continuous-wave (CW) vector network analyzer (VNA) spectroscopy is used to create two different models, both with a coefficient of determination ( $R^2$ ) of 0.97. One model is based on the theoretical response obtained by means of the Looyenga effective medium theory (EMT) model, while the other is based on measured data. Both models have been experimentally validated with root mean square error (RMSE) values of 0.4 and 0.35% respectively. These small estimation errors show the potential of this frequency range to design compact, cost-effective and in-line food moisture sensors. This research contributes to improving quality control and monitoring of moisture levels in flour-based mixtures.

**Index Terms**—food products, millimeter wave technology, modeling, moisture measurement, nondestructive testing, permittivity, scattering parameters, spectroscopy.

## I. INTRODUCTION

**N**OWADAYS, there is an increasing concern for the production of safe food for consumers. In this context, monitoring moisture content in food products is crucial to assess their quality and durability. The moisture content of a product directly influences its texture, mechanical strength, taste and microbial growth, thereby significantly impacting the quality and shelf-life of the final food material [1]. Another important parameter related to food quality is the water activity that represents the amount of free water

available for microbiological reactions with bacteria, yeasts and molds [2]. Although both water activity and total moisture content are closely related, this relationship is complex and depends on the specific food product [3]. Moisture content is usually expressed as a percentage of the total weight of a substance, representing the amount of water present. Water activity, on the other hand, is measured on a scale ranging from 0 to 1, with higher values indicating higher availability of free water. Moisture content and water activity must be lower than approximately 10% and 0.60-0.65 respectively in order to reduce the microbiological reactions of the food material [4].

There are different techniques to monitor food water content, which can be primarily categorized as direct or indirect approaches [5]. Direct techniques, such as gravimetric [6] and chemical methods [7], are usually destructive and time-consuming, and therefore they cannot be used in food production lines in order to measure water content in real time. Although indirect techniques need to measure an intermediate variable in order to estimate moisture content, which implies a previous calibration, they are often non-destructive and need a shorter measurement time. This makes them an ideal solution for in-line estimation of food moisture content [5]. Indirect techniques include conventional approaches, such as the resistance [8] and capacitance methods [9], nuclear magnetic resonance (NMR) [10], ultrasonic spectroscopy [11], [12], hygrometric methods [13], near infrared (NIR) spectroscopy [14], [15] and microwave [16-25], millimeter-wave [26] and terahertz (THz) approaches [27-31]. Among all of these indirect techniques, only microwave and millimeter-wave methods provide a contactless, non-destructive, cost-effective, instantaneous and in-line monitoring system with sufficient depth of penetration to obtain representative values of the total food moisture content [5]. The other two high-frequency techniques, i.e. NIR and THz spectroscopy, require expensive equipment and, in addition, the infrared approach features penetration depths in the micrometer range, leading to a poor representativeness of the total water content [32], [33]. The operating principle of these electromagnetic sensors [14-31] is based on the interaction of the food material with the applied electromagnetic field. As the magnetic response is negligible in most cases, this interaction is commonly quantified by the dielectric permittivity of the material, whose real part represents its ability to store the energy of the applied electric

<sup>M</sup>anuscript submitted June 1, 2023. This work was supported in part by the Spanish State Research Agency, Project No. PID2019-109984RBC43/AEI/10.13039/501100011033 and by the Government of Navarra under project IAFOOD, grant 0011-1411-2020-000024. (*Corresponding author: Carlos Quemada Mayoral*).

C. Q. Mayoral is with the Department of Statistics, Computer Science and Mathematics, Public University of Navarra, 31006 Pamplona, Spain (e-mail: [carlos.quemada@unavarra.es](mailto:carlos.quemada@unavarra.es)).

Iñigo Ederra, Miguel Beruete, Ramón Gonzalo and Juan Carlos Iriarte are with the Department of Electric, Electronic and Communications Engineering and with the Institute of Smart Cities, Public University of Navarra, 31006 Pamplona, Spain (e-mail: [inigo.ederra@unavarra.es](mailto:inigo.ederra@unavarra.es)).

> REPLACE THIS LINE WITH YOUR MANUSCRIPT ID NUMBER (DOUBLE-CLICK HERE TO EDIT) <

field and the imaginary part represents the electromagnetic energy converted into heat [22]. Due to the larger wavelength of the microwave devices used to monitor food moisture content, monitoring of small food products could be improper and inaccurate. For instance, the vacuum wavelength at a typical monitoring frequency of 2.45 GHz is 12.24 cm, much larger than the dimensions of most food products. In view of this shortcoming, the millimeter-wave range seems to be the best option in order to implement contactless, cost-effective and on-line sensors to monitor the water content of food products in the range of a few centimeters in any of their dimensions. In addition, the absorption coefficient of liquid water in the microwave and millimeter-wave ranges increases with frequency [34]. This makes the millimeter-wave range more sensitive to water content than the microwave range.

Food moisture content with millimeter waves has only been studied in [26], where a real-time, contactless and non-destructive sensor methodology to monitor the drying and freezing process of potato slabs by means of changes in the transmission coefficient of the samples in the 57-64 GHz frequency range was proposed. Considering the reduced thickness of the samples in this study (1.5 mm) and the comparatively smaller range of moisture variation than in reference [26], it is beneficial to decrease the radiation wavelength. This allows for more representative and accurate moisture results. Therefore, the operation frequency explored in this work spans from 67 to 110 GHz, as it offers smaller wavelengths than in [26] (5 mm at 60 GHz) to improve measurement accuracy. In addition, [26] does not present any model for estimating moisture content in food products.

In this work we analyze flour matrices and estimate their moisture content. To this aim, data obtained by continuous-wave (CW) vector network analyzer (VNA) transmission spectroscopy at millimeter-wave frequencies are used to create and validate two different estimation models, in which the resulting transmission levels through the samples are correlated with gravimetric water content. The proposed frequency range, 67-110 GHz, includes the automotive radar band (76-81 GHz), where fully integrated and off-the-shelf radar transceivers are being developed. Therefore, this frequency range represents a challenging and invaluable opportunity to design compact, cost-effective and in-line food moisture sensors. Due to the excellent agreement achieved in the correlation with gravimetric data, this work constitutes the first step towards the design of a contactless and cost-effective moisture sensor with millimeter waves directly applied to a food production line.

This paper is organized as follows. Section II introduces the most important theoretical aspects related to the permittivity calculation of materials composed of a mixture of different macroscopic components. Section III includes the measurement methodology and setup used in this experiment. Section IV presents the most remarkable experimental results together with the theoretical calculations and, finally, Section V concludes this research work.

## II. BACKGROUND

### A. Permittivity of Food Mixtures

Some foods such as vegetables, fruits and products derived from flour, among others, contain a significant amount of water. Because of its particular charge distribution, the water molecule possesses a permanent electric dipole moment and responds readily to the application of an electromagnetic field. On account of this, pure water in liquid phase has a dielectric constant significantly higher than other substances found in food products [35]. Because water is a strongly polar solvent for the frequency range considered in this work, permittivity of the food under test will be dominated by its water content, which in turn depends on the specific frequency, temperature and phase state [36], [37].

When the wavelength of the radiation used to characterize the sample is relatively long compared to its components, effective medium theory (EMT) models have been proven successful to estimate the sample permittivity on a macroscopic scale from the dielectric permittivity of each of its individual constituents. Among the different EMT models, it is possible to find approaches that develop different mathematical expressions depending on the geometry of the particles such as the Bruggeman model [38], [39]. On the other hand, other solutions such as the Birchak [40] and Looyenga [41] models do not consider the shape of the particles inside the composite. Since the main constituent of the food tested in this study is flour and its particles are irregular in shape and size, the first type of approach was directly discarded. Among the solutions included in the second group, Looyenga model is the one that best fits the experimental results obtained in this work. This model estimates the complex permittivity of the mixture ( $\epsilon$ ) by means of the following equation [41]:

$$\epsilon^{1/3} = \sum_{i=1}^n v_i (\epsilon_i)^{1/3}, \quad (1)$$

where  $v_i$  and  $\epsilon_i$  are the volume fraction and complex permittivity of the component  $i$  respectively. According to [42], the Looyenga model yields accurate enough estimations when the particles are larger than 50  $\mu\text{m}$ . In the samples used in this work, even though the granularity of the samples was not measured, given the similarity of the used flour with respect to [43], the particle size is estimated to be between 75 and 85  $\mu\text{m}$ .

In the specific case of this paper, the three main constituents of the food matrices under test are corn flour, liquid water and air. The complex permittivity of corn flour in the 67-110 GHz frequency range was experimentally estimated following the measurement procedure explained in Section II-B. The complex permittivity of pure water ( $\epsilon_w$ ) was estimated by using the single Debye model [44], expressed as:

$$\epsilon_w = \frac{\epsilon_0 - \epsilon_\infty}{1 - j(2\pi f\tau)} + \epsilon_\infty, \quad (2)$$

where  $f$  is the operating frequency in hertz,  $\epsilon_0$  and  $\epsilon_\infty$  are the static ( $f \rightarrow 0$ ) and high frequency ( $f \rightarrow \infty$ ) dielectric

> REPLACE THIS LINE WITH YOUR MANUSCRIPT ID NUMBER (DOUBLE-CLICK HERE TO EDIT) <

constants of pure water respectively and  $\tau$  is the relaxation time constant of pure water. As  $\epsilon_0$ ,  $\epsilon_\infty$  and  $\tau$  depend on temperature, the permittivity of pure water will be a complex value that depends both on temperature and frequency.

### B. Measurement of Complex Permittivity

Free-space measurement techniques constitute a simple and fast solution to estimate the dielectric properties of food materials. This method is particularly useful at millimeter-wave frequencies, as it overcomes the limitations posed by the small size of guided devices and resonant cavities. As shown in Fig. 1, the food sample is placed between two antennas for a non-contact and non-destructive measurement. Depending on the type of sample under test and the final application for which the sensor is intended, different setup configurations can be used, such as reflection [45], transmission [46] or reflection/transmission [47]. In the specific case of this work, the transmission configuration has been chosen.

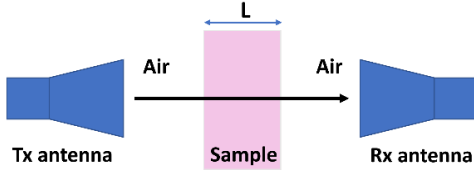


**Fig. 1.** Free-space measurement of complex permittivity.

The complex permittivity extraction performed in this study is based on the work by Duvillaret et al. [46]. We assume that the sample is a slide of homogeneous material of thickness  $L$  with two flat and parallel sides and magnetically isotropic with no surface charges and linear electromagnetic response. It is inserted between two media, which are air in this study. The sample is illuminated by a plane wave at normal incidence, whose polarization is linear. With these assumptions, the transmission coefficient ( $T(\omega) = S_{\text{sample}}(\omega)/S_{\text{ref}}(\omega)$ ) of the sample is obtained by dividing the spectral component of the electric field of the wave transmitted through the sample at the angular frequency  $\omega$  ( $S_{\text{sample}}(\omega)$ ) by the spectral component of the electric field transmitted without the sample at the same frequency  $\omega$  ( $S_{\text{ref}}(\omega)$ ). Assuming that the refractive index of the air is 1, the final expression of the complex transmission coefficient is as follows [46]:

$$T(\omega) = \frac{4\tilde{n}}{(\tilde{n} + 1)^2} \cdot e^{-i(\tilde{n}-1)\frac{\omega L}{c}} \cdot F(\omega), \quad (3)$$

where  $\tilde{n}$  is the complex refractive index of the sample,  $c$  is the speed of light in vacuum and  $F(\omega)$ , which represents the Fabry-Pérot effect inside the sample, is calculated as [46]:

$$F(\omega) = \frac{1}{1 - \left(\frac{\tilde{n} - 1}{\tilde{n} + 1}\right)^2 e^{-2i\tilde{n}\frac{\omega L}{c}}}. \quad (4)$$

For non-magnetic samples, such as corn flour,  $\tilde{n}$  is related to the relative permittivity of the sample  $\epsilon_r$  with the relation  $\tilde{n} = \sqrt{\epsilon_r}$ . In the specific case of this work,  $T(\omega)$  has been obtained by measuring the  $S_{21}$  parameter of the sample by means of a VNA using the setup described in Section III-B. Then, by using (3) inside an iterative process with an initial

value of  $\epsilon_r$  close to its real value, the final estimation for the relative permittivity of the sample is achieved.

## III. MEASUREMENT SETUP

### A. Sample Preparation

The two kinds of samples analyzed in this research work, corn flour and corn tortillas, are both industrial food products. The corn tortillas produced for this project correspond to four different water concentrations: 31, 35, 37.5 and 39.5%. These values correspond to standard water concentration levels found during production of commercial tortillas. Despite the nominal water concentration of each tortilla under test is known a priori, the moisture content of all samples has been determined by a gravimetric method. To this aim, all samples have been dehydrated inside an oven at about 60 °C for 24 hours. By weighing the samples just before the millimeter-wave measurement and just after the dehydration process, the estimation for the water content of each sample is obtained in order to detect possible errors in the initial nominal concentrations or losses of moisture in the transportation and storage processes. The same gravimetric technique has also been employed for the corn flour.

### B. S-Parameter Experimental Setup

The technique used to characterize the different samples of this work is the CW VNA spectroscopy. This method makes use of a VNA to obtain the scattering parameters of the sample under test within a broad bandwidth at millimeter-wave frequencies (67-110 GHz).

In our VNA based setup, a CW signal at microwave frequencies is generated by a microwave source included in the Agilent N5242A VNA. This signal is multiplied by non-linear devices (e.g., Schottky diodes) in order to convert it up to millimeter-wave frequencies. These non-linear devices are included in the VDI W-band VNA extenders. The average output power level is 2.5 dBm. By means of a 20 dBi standard gain horn antenna (Flann 27240-20), attached at the end of the transmitter extender, the beam is directed toward the antenna of the receiver extender after passing through the sample. The receiver antenna has the same technical characteristics as the transmitter antenna. At the receiver, a reverse process converts the signal into microwave frequencies before being introduced into the VNA again. In order to illuminate the sample, four 115 mm focal length plano-convex LAT100 lenses from Thorlabs Inc. are used to collimate the beam, two between the transmitter antenna and the sample and two others between the sample and the receiver antenna. The optimized symmetrical distances between the antenna and the first lens, between both lenses and between the second lens and the sample are 92.2, 190 and 92.2 mm respectively, which correspond to  $f$ ,  $2f$  and  $f$ , being  $f$  the focal length. The beamwidth of the beam spot generated at the sample position ranges from 17 mm at 75 GHz to 19 mm at 110 GHz. Before starting the characterization process, a measurement without the sample is carried out to calibrate the measurement setup. Fig. 2 shows a detailed photograph of the used measurement system.

> REPLACE THIS LINE WITH YOUR MANUSCRIPT ID NUMBER (DOUBLE-CLICK HERE TO EDIT) <

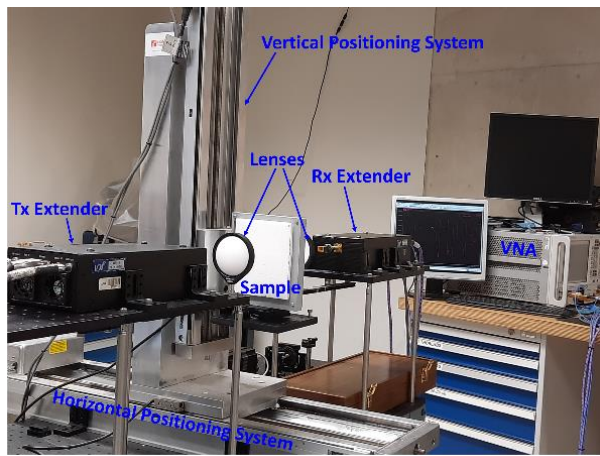


**Fig. 2.** Measurement Setup.

To position the samples, a 180 mm × 155 mm × 19 mm rectangular 3D-printed holder was designed to house inside the sample under test. Since different parts of a tortilla may differ slightly in terms of water concentration, flatness and roughness, an XY sample positioning system was used in order to measure the  $S_{21}$  parameter at different points of the sample. This is achieved by using two precision step motors. In total, the  $S_{21}$  parameter was monitored at 81 points of each tortilla and the average of all these values is calculated and recorded as the final datum of the sample. With the objective of keeping the sample flat and perpendicular to the beam and after checking that the influence of the expanded polystyrene on the measurement process is negligible, the sample was sandwiched between two 0.5 cm thick sheets of this material. This can be seen in Fig. 3.

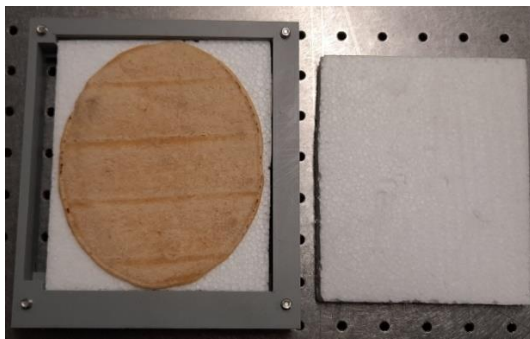


**Fig. 3.** 3D-Printed holder together with the sample and the two sheets of expanded polystyrene. Each tortilla is approximately an ellipse of semi-axes 7 and 5.8 cm, and thickness 1.5 mm.

In the case of the corn flour, a rectangular case of expanded polystyrene was used to house inside the sample, which was compressed before the measurement in order to remove some of the air inside it. According to the dimensions of this case, the beam passes through a thickness of flour of about 23 mm. Even though in this case a rectangular container was used any geometry that keeps the sample limited by two flat surfaces and illuminated at normal incidence, and whose size allows the radiation beam to be completely contained in the sample, could be used.

## IV. RESULTS

### A. Corn Flour Dielectric Constant

The starting point for the estimation of the dielectric constant of the flour matrices is the determination of the flour dielectric constant. Since no permittivity measurements were found in the literature for corn flour at the working frequency range, its complex permittivity was determined experimentally by means of the method described in Section II-B. The resulting real ( $\epsilon'_r$ ) and imaginary ( $\epsilon''_r$ ) parts are shown in Fig. 4. This measurement was performed by means of the setup described in Section II-B, in which the selected corn flour featured a moisture of 8.4% at 22 °C. This value was estimated by thermogravimetric techniques, heating the sample at about 60 °C for 24 hours. As shown in Fig. 4, the relative permittivity is nearly constant, being the average value of its real and imaginary parts around 2.26 and 0.15 respectively.

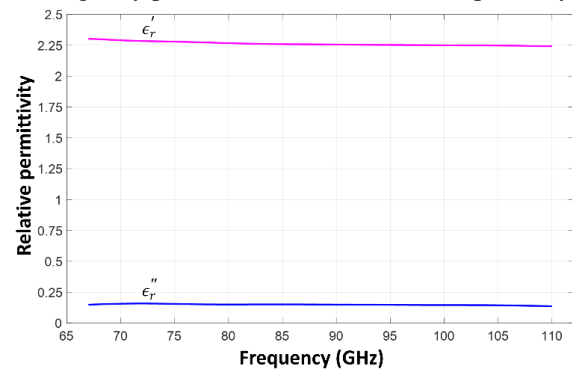


**Fig. 4.** Real ( $\epsilon'_r$ ) and imaginary ( $\epsilon''_r$ ) parts of the experimentally measured relative permittivity of the corn flour used to produce the tortillas.

### B. Sample Moisture Estimation

By incorporating the obtained relative permittivity of the corn flour, the weight measurements of each tortilla before and after dehydration, the moisture content of the corn flour, the total volume of each tortilla and the complex permittivity of pure water as described in Section II-A, the complex dielectric constant of each tortilla can be derived from (1). It is important to note that the relative permittivity of air is assumed to be 1, and the volume fraction of air in each tortilla is approximately 0.32 [48]. This value averages the air gaps in the tortillas. Concerning the calculation of the total volume of each sample, the same value has been used for all of them, assuming that each tortilla is approximately an ellipse of semi-axes 7 cm and 5.8 cm, and thickness 1.5 mm.

Once the relative permittivity of a tortilla has been estimated, the corresponding  $S_{11}$  and  $S_{21}$  parameters can be obtained by [49]:

$$S_{11} = \frac{\Gamma(1 - T^2)}{1 - \Gamma^2 T^2}, \quad (5)$$

$$S_{21} = \frac{T(1 - \Gamma^2)}{1 - \Gamma^2 T^2}, \quad (6)$$

where  $T$  is the transmission coefficient inside the tortilla and  $\Gamma$  is the reflection coefficient in the air-sample interface for a



> REPLACE THIS LINE WITH YOUR MANUSCRIPT ID NUMBER (DOUBLE-CLICK HERE TO EDIT) <

normally incident plane wave, given by [49]:

$$T = e^{-\gamma d}, \quad (7)$$

$$\Gamma = \frac{(1 - \sqrt{\epsilon_r})}{(1 + \sqrt{\epsilon_r})}, \quad (8)$$

where  $d$  is the sample thickness and  $\gamma$  is the complex propagation constant [49]:

$$\gamma = \frac{j2\pi f}{c} \sqrt{\epsilon_r}. \quad (9)$$

Note that equation (6) is equivalent to (3), but this new formulation is considered in order to include the information about the reflection caused by the samples.

The theoretical  $S_{21}$  values calculated following this method are then compared with the experimental results in order to obtain a moisture content estimation model.

As an example, Fig. 5 shows the theoretical and experimental values of the magnitude of  $S_{21}$  for a sample of each moisture concentration as a function of frequency.

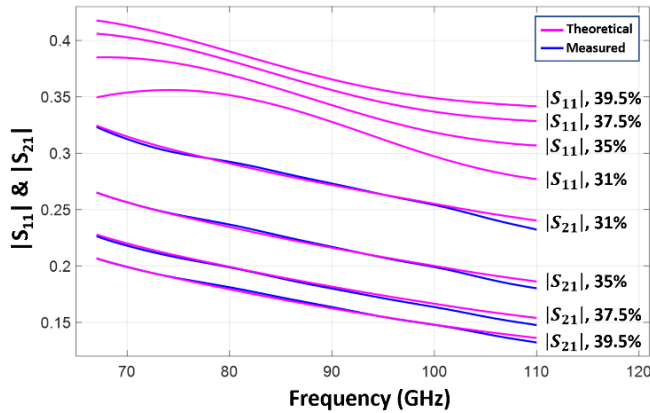


**Fig. 5.** Theoretical and measured values of  $|S_{11}|$  and  $|S_{21}|$  for a tortilla of each nominal moisture concentration.

As indicated in Fig. 5, both the theoretical value and the measured value of  $|S_{21}|$  decrease with frequency and show satisfactory agreement over the whole frequency range. If the theoretical value of  $|S_{11}|$  is represented too, it can be noticed that it also decreases with frequency. This means that both the reflectance and transmittance decrease with frequency, indicating that the absorbed power increases with frequency. This power absorption at millimeter-wave frequencies is mainly caused by the water contained in the tortilla and, more specifically, by its relatively high  $\epsilon_r''$  value (18.53 at 67 GHz and 22 °C according to (2) for the 35% moisture sample). This result has been verified with the electromagnetic simulation software CST Studio Suite, taking as input the complex permittivity of the 35% moisture tortilla calculated by (1). Fig. 6 presents  $|S_{11}|$  and  $|S_{21}|$ , and the absorbance calculated as  $A(f) = 1 - |S_{11}|^2 - |S_{21}|^2$ , where  $|S_{11}|^2$  represents the reflectance and  $|S_{21}|^2$  the transmittance. The values of  $|S_{11}|$  and  $|S_{21}|$  are the same as the ones in Fig. 5 and show that the absorbance also increases with frequency as mentioned above.

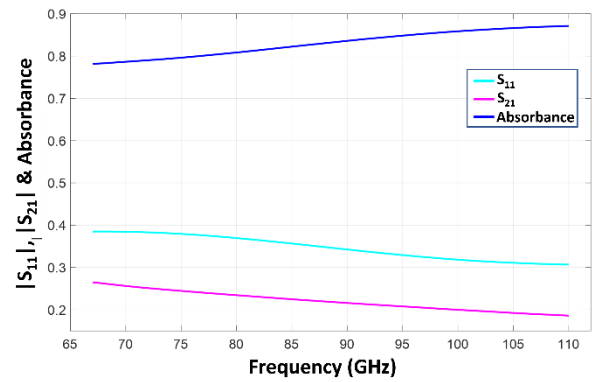


**Fig. 6.** Theoretical values of  $|S_{11}|$ ,  $|S_{21}|$  and absorbance only for the 35% moisture sample of those represented in Fig. 5 obtained by means of the electromagnetic simulation software CST Studio Suite.

Based on the experimental results of transmission through the samples and on the theoretical results obtained by using (6), two different models have been created for moisture content estimation. The first model, depicted in Section IV-C, is obtained by means of the theoretical  $S_{21}$  of all tortillas at a specific frequency, and then compared to the measured  $S_{21}$  at the same frequency. To create the second model, presented in Section IV-D, the sample space is divided into two groups of 24 and 16 tortillas. The first group is used to create the model and the second group to validate it.

### C. Model Based on Theoretical Data

The first model to evaluate the moisture content of flour matrices is based on the theoretical model for complex permittivity described in Section II, whose value allows the calculation of the  $S_{21}$  parameter by means of (6).

To start with, the magnitude of the  $S_{21}$  parameter measured for each sample at 67, 90 and 110 GHz is correlated with its water content measured by thermogravimetric techniques and the result is shown in Fig. 7.

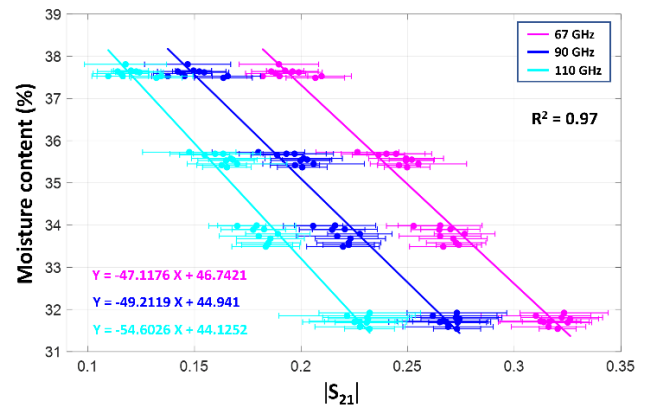


**Fig. 7.** Scatter plot of  $|S_{21}|$  measured for each sample at 67, 90 and 110 GHz and its moisture content measured by thermogravimetric techniques. Note that each value of  $|S_{21}|$  corresponds to the average value of this parameter measured at 81 points of each sample. The standard deviation of  $|S_{21}|$  has been included as an error bar for each sample. The largest standard deviation is 0.032.

> REPLACE THIS LINE WITH YOUR MANUSCRIPT ID NUMBER (DOUBLE-CLICK HERE TO EDIT) <

As shown in Fig. 7,  $|S_{21}|$  is well correlated to moisture content with a coefficient of determination ( $R^2$ ) of about 0.97 for the three considered frequencies. These results also confirm the inversely proportional relationship between both magnitudes. The lower the moisture content of the sample, the lower its absorbance and the higher its transmittance. In addition, as discussed in Fig. 5, for a fixed moisture percentage, the magnitude of  $S_{21}$  decreases with frequency.

Fig. 8 shows the magnitude of the theoretical  $S_{21}$  parameter estimated at 77 GHz by (6) for each sample and correlated with its water content measured by thermogravimetric techniques. In addition, the measured values of  $|S_{21}|$  at the same frequency for each tortilla are also represented.

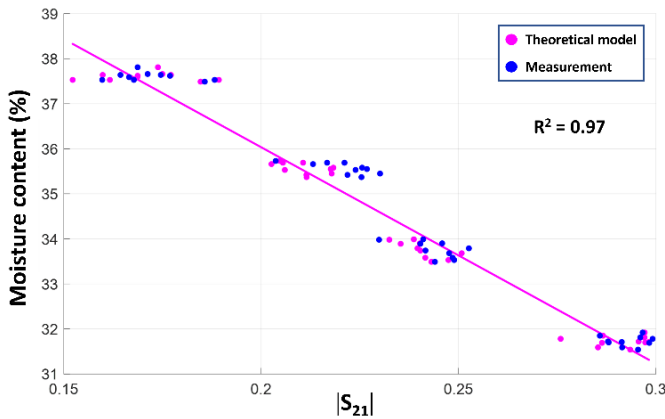


**Fig. 8.** Scatter plot of the magnitude of the theoretical and measured  $S_{21}$  parameter at 77 GHz for each sample and its moisture content measured by thermogravimetric techniques.

By using the theoretical data of Fig. 8, a model that enables the estimation of the water content of a corn tortilla from the value of  $|S_{21}|$  calculated by (6) at 77 GHz has been created with a coefficient of determination of approximately 0.97. If the measured data are used to validate the model, a root mean square error (RMSE) of about 0.4% is achieved.

In the measurement process of each sample, the value of  $|S_{21}|$  corresponds to the average value of this parameter measured at 81 points of the sample under test. Each sample has been measured only once since it has been found that the maximum standard deviation due to the repeatability of the measurement of a sample is negligible compared to the standard deviation due to the measurement of the same sample in 81 different points. This is due to the use of a rigid sample holder and a very accurate micrometer positioning system. Fig. 9 shows the measurement of 8 tortillas at 67, 90 and 110 GHz, two of each nominal moisture concentration, each measured 5 times. It can be observed that the variations of  $|S_{21}|$  in the repeatability measurements of the same sample are almost imperceptible. Table I shows the mean and standard deviation of the measurements performed at 90 GHz. When comparing the maximum standard deviation of these measurements with the maximum standard deviation due to the measurement at the 81 points in each sample (0.032), it becomes evident that the variations generated by repeatability are approximately 100 times smaller.

**TABLE I**  
MEAN AND STANDARD DEVIATION OF REPEATABILITY MEASUREMENTS AT 90 GHZ

Sample	1	2	3	4	5	6	7	8
Mean	0.165	0.164	0.187	0.186	0.217	0.223	0.272	0.274
STD/ $10^{-4}$	2.89	1.49	3.18	3.08	2.09	1.39	3.19	2.19

Abbreviations: STD: Standard deviation.

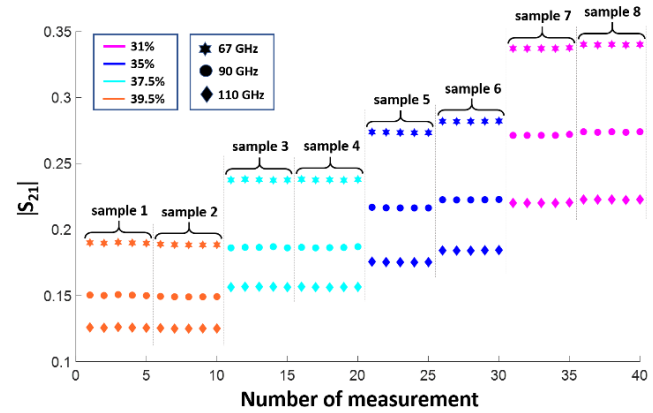


**Fig. 9.** Scatter plot of  $|S_{21}|$  repeatability measurements of 8 samples at 67, 90 and 110 GHz, two of each nominal moisture concentration, each measured 5 times. Note that each value of  $|S_{21}|$  corresponds to the average value of this parameter measured at 81 points of each sample.

#### D. Model Based on Experimental Data

The second proposed model relies only on measured data. The same data used to validate the previous model at 77 GHz will now be used to build and validate the experimental model. These results are correlated with gravimetric water content and presented in Fig. 10.

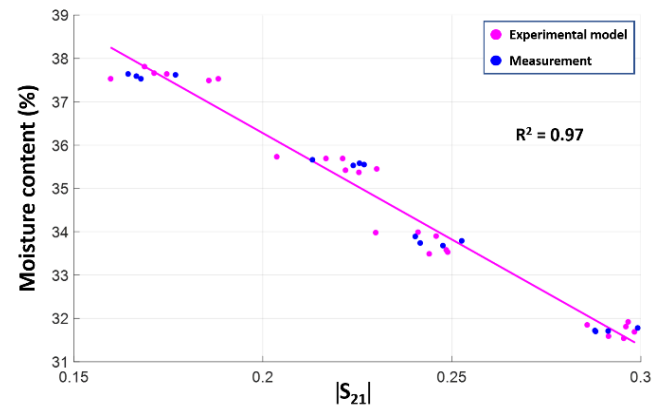


**Fig. 10.** Scatter plot of the magnitude of the  $S_{21}$  parameter measured at 77 GHz for each sample and its moisture content measured by thermogravimetric techniques. Note that each value of  $S_{21}$  corresponds to the average value of this parameter measured at 81 points of each sample.

> REPLACE THIS LINE WITH YOUR MANUSCRIPT ID NUMBER (DOUBLE-CLICK HERE TO EDIT) <

In order to create a model based on these experimental data, a variant of the Kennard-Stone algorithm [50] has been used by eliminating the samples selected to build the model between each iteration and the next and dividing the sample space into four subsets by nominal moisture content. As the samples are selected in pairs, it has been necessary to choose 24 samples to create the model and 16 samples for its validation. With the selected samples, a model based on experimental data is achieved with a coefficient of determination of about 0.97. This model allows the estimation of the water content of a corn tortilla from the value of  $|S_{21}|$  measured at 77 GHz. If the remaining data of Fig. 10 are used to validate the model, a value for RMSE of approximately 0.35% is obtained.

Table II shows a comparison of this work with other state-of-the-art references. The first columns indicate whether or not the technologies used satisfy certain relevant properties: non-destructive, contactless, in-line, real-time and low-cost. The last two columns compare this work with the other references by using two factors of merit, the coefficient of determination ( $R^2$ ) and the estimation error. Although the comparison of the prediction error of the direct techniques with the indirect ones does not make sense since the indirect techniques make use of an intermediate variable to estimate the moisture content, if the comparison is focused only on the indirect techniques, it is worth mentioning that the two factors of merit for this study are similar to the values established by the state of the art.

## V. CONCLUSIONS

This experimental study concludes that it is possible to estimate the moisture content of flour matrices with an RMSE lower than 0.5% by using CW-VNA spectroscopy at millimeter-wave frequencies (67-110 GHz). In order to perform this estimation, two different models have been developed, one based on purely experimental data and the other completely theoretical, achieving a lower validation error (0.35%) for the first one.

The theoretical model first estimates the relative permittivity of each sample by using the Looyenga model, one of the EMT models to estimate the sample permittivity on a macroscopic scale from the dielectric permittivity of each of its individual constituents. Among these constituents, the dielectric constant of the flour must be determined. It has been shown that, for the analyzed corn tortillas, the dielectric constant of the corn flour can be obtained by millimeter-wave spectroscopy. From this value, the  $S_{21}$  transmission parameter can be calculated for different moisture levels and high correlation with its gravimetric moisture content can be found.

The small estimation errors achieved in this study pave the way towards the use of millimeter-wave frequencies to estimate the moisture content of food products. The development of cost-effective and in-line food moisture sensors can be facilitated by the already, off-the-shelf and fully-integrated automotive radar transceivers at 77 GHz.

TABLE II  
COMPARISON OF THIS WORK WITH OTHER REFERENCES

Ref.	Technique	Non-destructive	Contactless	In-line	Real-time	Low-cost	$R^2$	Error
[6]	Gravimetric					✓*	N/A	RE = 0.37%
[7]	Chemical						N/A	RE = 0.19%
[9]	Capacitive	✓		✓	✓	✓	0.98	RMSE = 0.71%
[10]	NMR	✓	✓				0.99	N/A
[11]	Ultrasonic	✓		✓	✓	✓	0.9	N/A
[14]	NIR spectroscopy	✓	✓	✓	✓		0.92	RMSE = 0.48%
[20]	Microwave	✓	✓	✓	✓	✓	0.98	RMSE = 2%
[26]	Millimeter-wave	✓	✓	✓	✓		N/A	N/A
[27]	Terahertz TDS	✓	✓	✓	✓		0.97	RMSE = 2.2%
<b>This work</b>	Millimeter-wave	✓	✓	✓	✓		0.97	RMSE = 0.35%

\*: Cost is lower than for other techniques but depends on the degree of precision to be achieved.

✓: It indicates that the technique satisfies the specific property.

Abbreviations: NIR: Near infrared, NMR: Nuclear magnetic resonance, RE: Relative Error, RMSE: Root mean square error, TDS: Time-domain spectroscopy.

## REFERENCES

- [1] L. Afsah-Hejri, P. Hajeb, P. Ara, and R. J. Ehsani, "A Comprehensive Review on Food Applications of Terahertz Spectroscopy and Imaging," *Compr. Rev. Food Sci. Food Saf.*, vol. 18, no. 5, pp. 1563–1621, Sep. 2019, doi: <https://doi.org/10.1111/1541-4337.12490>.
- [2] T. Hinz, F. Menke, R. Eggers, and R. Knöchel, "Development of a Microwave Moisture Sensor for Application in the Food Industry," *LWT - Food Sci. Technol.*, vol. 29, no. 4, pp. 316–325, 1996, doi: <https://doi.org/10.1006/food.1996.0048>.
- [3] M. Mathlouthi, "Water content, water activity, water structure and the stability of foodstuffs," *Food Control*, vol. 12, no. 7, pp. 409–417, 2001, doi: [https://doi.org/10.1016/S0956-7135\(01\)00032-9](https://doi.org/10.1016/S0956-7135(01)00032-9).
- [4] D. G. Mercer, "Solar Drying in Developing Countries : Possibilities and Pitfalls," in *Using food science and technology to improve nutrition and promote national development*, G. Robertson and J. Lupien, Eds. 2008.
- [5] M. Vera Zambrano, B. Dutta, D. G. Mercer, H. L. MacLean, and M. F. Touchie, "Assessment of moisture content measurement methods of dried food products in small-scale operations in developing countries: A review," *Trends Food Sci. Technol.*, vol. 88, pp. 484–496, 2019, doi: <https://doi.org/10.1016/j.tifs.2019.04.006>.
- [6] H. Roozendaal, M. Abu-hardan, and R. A. Frazier, "Thermogravimetric analysis of water release from wheat flour and wheat bran suspensions," *J. Food Eng.*, vol. 111, no. 4, pp. 606–611, 2012, doi: <https://doi.org/10.1016/j.jfoodeng.2012.03.009>.
- [7] H.-D. Isengard and P. Heinze, "Determination of total water and surface water in sugars," *Food Chem.*, vol. 82, no. 1, pp. 169–172,

> REPLACE THIS LINE WITH YOUR MANUSCRIPT ID NUMBER (DOUBLE-CLICK HERE TO EDIT) <

- 2003, doi: [https://doi.org/10.1016/S0308-8146\(02\)00540-X](https://doi.org/10.1016/S0308-8146(02)00540-X).
- [8] G. O. I. Ezeike, "A resistive probe moisture sensor for tropical root crops and vegetables," *J. Agric. Eng. Res.*, vol. 37, no. 1, pp. 15–26, 1987, doi: [https://doi.org/10.1016/0021-8634\(87\)90128-4](https://doi.org/10.1016/0021-8634(87)90128-4).
- [9] C. V. Kandala and J. Sundaram, "Nondestructive Measurement of Moisture Content Using a Parallel-Plate Capacitance Sensor for Grain and Nuts," *IEEE Sens. J.*, vol. 10, no. 7, pp. 1282–1287, 2010, doi: [10.1109/JSEN.2010.2041446](https://doi.org/10.1109/JSEN.2010.2041446).
- [10] H. Hickey, B. MacMillan, B. Newling, M. Ramesh, P. Van Eijck, and B. Balcom, "Magnetic resonance relaxation measurements to determine oil and water content in fried foods," *Food Res. Int.*, vol. 39, no. 5, pp. 612–618, 2006, doi: <https://doi.org/10.1016/j.foodres.2005.12.007>.
- [11] M. Contreras, J. Benedito, and J. V. Garcia-Perez, "Ultrasonic characterization of salt, moisture and texture modifications in dry-cured ham during post-salting," *Meat Sci.*, vol. 172, p. 108356, 2021, doi: <https://doi.org/10.1016/j.meatsci.2020.108356>.
- [12] J. V. Garcia-Perez, M. de Prados, G. Martinez, T. E. Gomez Alvarez-Arenas, and J. Benedito, "Ultrasonic online monitoring of the ham salting process. Methods for signal analysis: Time of flight calculation," *J. Food Eng.*, vol. 263, pp. 87–95, 2019, doi: <https://doi.org/10.1016/j.jfoodeng.2019.05.032>.
- [13] B. A. Prior, "Measurement of Water Activity in Foods: A Review," *J. Food Prot.*, vol. 42, no. 8, pp. 668–674, 1979.
- [14] G. Mishra, S. Srivastava, B. K. Panda, and H. N. Mishra, "Rapid Assessment of Quality Change and Insect Infestation in Stored Wheat Grain Using FT-NIR Spectroscopy and Chemometrics," *Food Anal. Methods*, vol. 11, no. 4, pp. 1189–1198, 2018, doi: [10.1007/s12161-017-1094-9](https://doi.org/10.1007/s12161-017-1094-9).
- [15] M. M. Tripathi, E. B. M. Hassan, F.-Y. Yueh, J. P. Singh, P. H. Steele, and L. L. Ingram, "Reflection-absorption-based near infrared spectroscopy for predicting water content in bio-oil," *Sensors Actuators B Chem.*, vol. 136, no. 1, pp. 20–25, 2009, doi: <https://doi.org/10.1016/j.snb.2008.10.055>.
- [16] M. T. Jilani, M. Z. U. Rehman, A. M. Khan, O. Chughtai, M. A. Abbas, and M. T. Khan, "An implementation of IoT-based microwave sensing system for the evaluation of tissues moisture," *Microelectronics J.*, vol. 88, pp. 117–127, 2019, doi: <https://doi.org/10.1016/j.mejo.2018.03.006>.
- [17] S. G. Bjarnadottir, K. Lunde, O. Alvseike, A. Mason, and A. I. Al-Shamma'a, "Assessing Water Activity in Dry-Cured Ham using Microwave Spectroscopy," *Int. J. Smart Sens. Intell. Syst.*, vol. 7, pp. 1–4, 2020.
- [18] Z. Li, Z. Meng, A. Haigh, P. Wang, and A. Gibson, "Characterisation of water in honey using a microwave cylindrical cavity resonator sensor," *J. Food Eng.*, vol. 292, p. 110373, 2021, doi: <https://doi.org/10.1016/j.jfoodeng.2020.110373>.
- [19] M. A. Lewis, S. Trabelsi, and S. O. Nelson, "Development of an Eighth-scale Grain Drying System with Real-time Microwave Monitoring of Moisture Content," *Appl. Eng. Agric.*, 2019.
- [20] J. Zhang, D. Du, Y. Bao, J. Wang, and Z. Wei, "Development of Multifrequency-Swept Microwave Sensing System for Moisture Measurement of Sweet Corn With Deep Neural Network," *IEEE Trans. Instrum. Meas.*, vol. 69, no. 9, pp. 6446–6454, 2020, doi: [10.1109/TIM.2020.2972655](https://doi.org/10.1109/TIM.2020.2972655).
- [21] A. a H. Al-Muhtaseb, M. A. Hararah, E. K. Megahey, W. A. M. McMinn, and T. R. A. Magee, "Dielectric properties of microwave-baked cake and its constituents over a frequency range of 0.915–2.450 GHz," *J. Food Eng.*, vol. 98, pp. 84–92, 2010.
- [22] K. Solyom, P. Lopez, P. Esquivel, A. Lucia, and A. Vásquez-Caicedo, "Effect of temperature and moisture contents on dielectric properties at 2.45 GHz of fruit and vegetable processing by-products," *RSC Adv.*, vol. 10, pp. 16783–16790, Apr. 2020, doi: [10.1039/C9RA10639A](https://doi.org/10.1039/C9RA10639A).
- [23] Z. Li, A. Haigh, C. Soutis, A. Gibson, and R. Sloan, "Evaluation of added water content in honey using microwave transmission line technique," 2017.
- [24] C. Li, X. Yu, Z. Chen, Q. Song, and Y. Xu, "Free space traveling-standing wave attenuation method for microwave sensing of grain moisture content," *Meas. Control*, vol. 54, pp. 336–345, 2020.
- [25] J. Zhang, Y. Bao, D. Du, J. Wang, and Z. Wei, "OM2S2: On-Line Moisture-Sensing System Using Multifrequency Microwave Signals Optimized by a Two-Stage Frequency Selection Framework," *IEEE Trans. Ind. Electron.*, vol. 68, no. 11, pp. 11501–11510, 2021, doi: [10.1109/TIE.2020.3032927](https://doi.org/10.1109/TIE.2020.3032927).
- [26] G. Pandey, W. Vandermeiren, L. Dimiccoli, and J. Stiens, "Contactless monitoring of food drying and freezing processes with millimeter waves," *J. Food Eng.*, vol. 226, pp. 1–8, 2018, doi: <https://doi.org/10.1016/j.jfoodeng.2018.01.003>.
- [27] Y. Ren, T. Lei, and D.-W. Sun, "In-situ indirect measurements of real-time moisture contents during microwave vacuum drying of beef and carrot slices using terahertz time-domain spectroscopy," *Food Chem.*, vol. 418, p. 135943, 2023, doi: <https://doi.org/10.1016/j.foodchem.2023.135943>.
- [28] P. Parasoglou *et al.*, "Quantitative Water Content Measurements in Food Wafers Using Terahertz Radiation," 2010.
- [29] H. S. Chua *et al.*, "Terahertz time-domain spectroscopy of crushed wheat grain," in *IEEE MTT-S International Microwave Symposium Digest, 2005.*, 2005, pp. 2103–2106, doi: [10.1109/MWSYM.2005.1517162](https://doi.org/10.1109/MWSYM.2005.1517162).
- [30] L. Afsah Hejri, P. Hajeb, P. Ara, and R. Ehsani, "A Comprehensive Review on Food Applications of Terahertz Spectroscopy and Imaging," *Compr. Rev. Food Sci. Food Saf.*, vol. 18, no. 5, pp. 1563–1621, Aug. 2019, doi: [10.1111/1541-4337.12490](https://doi.org/10.1111/1541-4337.12490).
- [31] J. F. Federici, "Review of Moisture and Liquid Detection and Mapping using Terahertz Imaging," *J. Infrared, Millimeter, Terahertz Waves*, vol. 33, no. 2, pp. 97–126, 2012, doi: [10.1007/s10762-011-9865-7](https://doi.org/10.1007/s10762-011-9865-7).
- [32] S. Julrat and S. Trabelsi, "Measuring Dielectric Properties for Sensing Foreign Material in Peanuts," *IEEE Sens. J.*, vol. 19, no. 5, pp. 1756–1766, 2019, doi: [10.1109/JSEN.2018.2882367](https://doi.org/10.1109/JSEN.2018.2882367).
- [33] J. Peters *et al.*, "Design, development and method validation of a novel multi-resonance microwave sensor for moisture measurement," *Anal. Chim. Acta*, vol. 961, pp. 119–127, 2017, doi: <https://doi.org/10.1016/j.aca.2017.01.021>.
- [34] U. Møller, D. G. Cooke, K. Tanaka, and P. U. Jepsen, "Terahertz reflection spectroscopy of Debye relaxation in polar liquids [Invited]," *J. Opt. Soc. Am. B*, vol. 26, no. 9, pp. A113–A125, Sep. 2009, doi: [10.1364/JOSAB.26.00A113](https://doi.org/10.1364/JOSAB.26.00A113).
- [35] K. Kupfer, *Electromagnetic aquametry: Electromagnetic wave interaction with water and moist substances*. Springer, 2005.
- [36] S. O. Nelson, "Dielectric properties of agricultural products-measurements and applications," *IEEE Trans. Electr. Insul.*, vol. 26, no. 5, pp. 845–869, 1991, doi: [10.1109/14.99097](https://doi.org/10.1109/14.99097).
- [37] S. Ryyänen, "The electromagnetic properties of food materials: A review of the basic principles," *J. Food Eng.*, vol. 26, no. 4, pp. 409–429, 1995, doi: [https://doi.org/10.1016/0260-8774\(94\)00063-F](https://doi.org/10.1016/0260-8774(94)00063-F).
- [38] D. A. G. Bruggeman, "Berechnung verschiedener physikalischer Konstanten von heterogenen Substanzen. I. Dielektrizitätskonstanten und Leitfähigkeiten der Mischkörper aus isotropen Substanzen," *Ann. Phys.*, vol. 416, no. 7, pp. 636–664, Jan. 1935, doi: <https://doi.org/10.1002/andp.19354160705>.
- [39] D. A. G. Bruggeman, "Berechnung verschiedener physikalischer Konstanten von heterogenen Substanzen. II. Dielektrizitätskonstanten und Leitfähigkeiten von Vielkristallen der nichtregulären Systeme," *Ann. Phys.*, vol. 417, no. 7, pp. 645–672, Jan. 1936, doi: <https://doi.org/10.1002/andp.19364170706>.
- [40] J. R. Birchak, C. G. Gardner, J. E. Hipp, and J. M. Victor, "High dielectric constant microwave probes for sensing soil moisture," 1974.
- [41] H. Looyenga, "Dielectric constants of heterogeneous mixtures," *Physica*, vol. 31, no. 3, pp. 401–406, 1965, doi: [https://doi.org/10.1016/0031-8914\(65\)90045-5](https://doi.org/10.1016/0031-8914(65)90045-5).
- [42] D. C. Dube, "Study of Landau-Lifshitz-Looyenga's formula for dielectric correlation between powder and bulk," *J. Phys. D: Appl. Phys.*, vol. 3, no. 11, p. 1648, 1970, doi: [10.1088/0022-3727/3/11/313](https://doi.org/10.1088/0022-3727/3/11/313).
- [43] E. de la Hera, M. Talegón, P. Caballero, and M. Gómez, "Influence of maize flour particle size on gluten-free breadmaking," *J. Sci. Food Agric.*, vol. 93, no. 4, pp. 924–932, Mar. 2013, doi: <https://doi.org/10.1002/jsfa.6111>.



> REPLACE THIS LINE WITH YOUR MANUSCRIPT ID NUMBER (DOUBLE-CLICK HERE TO EDIT) <

- <https://doi.org/10.1002/jsfa.5826>.
- [44] H. J. Liebe, G. A. Hufford, and T. Manabe, "A model for the complex permittivity of water at frequencies below 1 THz," *Int. J. Infrared Millimeter Waves*, vol. 12, no. 7, pp. 659–675, 1991, doi: 10.1007/BF01008897.
- [45] C. Yang, H. Huang, and M. Peng, "Non-Iterative Method for Extracting Complex Permittivity and Thickness of Materials From Reflection-Only Measurements," *IEEE Trans. Instrum. Meas.*, vol. 71, pp. 1–8, 2022, doi: 10.1109/TIM.2022.3171514.
- [46] L. Duvillaret, F. Garet, and J.-L. Coutaz, "A reliable method for extraction of material parameters in terahertz time-domain spectroscopy," *IEEE J. Sel. Top. Quantum Electron.*, vol. 2, no. 3, pp. 739–746, 1996, doi: 10.1109/2944.571775.
- [47] A. M. Nicolson and G. F. Ross, "Measurement of the Intrinsic Properties of Materials by Time-Domain Techniques," *IEEE Trans. Instrum. Meas.*, vol. 19, no. 4, pp. 377–382, 1970, doi: 10.1109/TIM.1970.4313932.
- [48] M. L. Kawas and R. G. Moreira, "Characterization of product quality attributes of tortilla chips during the frying process," *J. Food Eng.*, vol. 47, no. 2, pp. 97–107, 2001, doi: [https://doi.org/10.1016/S0260-8774\(00\)00104-7](https://doi.org/10.1016/S0260-8774(00)00104-7).
- [49] D. K. Ghodgaonkar, V. V. Varadan, and V. K. Varadan, "Free-space measurement of complex permittivity and complex permeability of magnetic materials at microwave frequencies," *IEEE Trans. Instrum. Meas.*, vol. 39, no. 2, pp. 387–394, 1990, doi: 10.1109/19.52520.
- [50] R. W. Kennard and L. A. Stone, "Computer Aided Design of Experiments," *Technometrics*, vol. 11, no. 1, pp. 137–148, Feb. 1969, doi: 10.1080/00401706.1969.10490666.